JOURNAL OF Applied Polymer SCIENCE

Preparation and Evaluation of Composite Microspheres of Polyacrylamide-Grafted Polysaccharides

Rahul Tripathi, Brahmeshwar Mishra
Department of Pharmaceutics, Indian Institute of Technology, Banaras Hindu University, Varanasi 221 005, India
Correspondence to: B. Mishra (E-mail: bmishrabhu@rediffmail.com)

ABSTRACT: The poor mechanical strength and instability of polysaccharide's gel takes away opportunities for versatile application. The grafting of polyacrylamide (PAM) onto polysaccharide was found to be an efficient tool for transforming its properties and obtaining stable and robust composite microspheres (CMs). In this study, free-radical polymerization reaction was used for the grafting of PAM onto the polysaccharide backbone, and their hydrogel CMs were obtained through an ionotropic gelation method. Porous and buoyant CMs were obtained through the incorporation of sodium bicarbonate into the reaction mixture. Characterizations were done through Fourier transform infrared spectroscopy, thermal and scanning electron microscopy analysis. The mechanical strength and squeezing capacity were evaluated extensively through a modified syringe method developed in-house. The squeezing capacity of grafted CMs diminished with the formation of a complex interpenetrating network. The Young's modulus, swelling kinetics, mechanical strength, and squeezing capacity of the grafted microspheres were compared extensively. © 2013 Wiley Periodicals, Inc. J. Appl. Polym. Sci. 130: 2912–2922, 2013

KEYWORDS: biopolymers and renewable polymers; mechanical properties; synthesis and processing

Received 3 October 2012; accepted 18 April 2013; Published online 13 June 2013
DOI: 10.1002/app.39427

INTRODUCTION

Psyllium (Psy; *Plantago ovata Forsk*) is an annual plant grown primarily in India. Complex heteroxylans (the monosaccharides arabinose and xylose, the combination of which is referred to as *arabinoxylan*) are the most abundant polysaccharide in Psy. Arabinofuranose, rhamnose, and xylopyranose monosaccharide residues are attached at positions 2 and 3, respectively, on the main chain of Psy.[1–3]

Sodium alginate (NaAlg) is a linear polysaccharide that is cellulosic in nature and made up of (1,4)-β-D-mannuronate and (1,3)-α-L-guluronate sugar subunits with carboxylic groups in every repeating unit and has α and β configurations. NaAlg is obtained from marine brown algae made up of three different types of polymer segments: poly(β-D-mannopyranosyluronate), poly(α-L-gulupyranosyluronate), and a segment with alternating sugar units.[4,5] These polysaccharides are very susceptible to chemical, thermal, and mechanical degradation; also, gel formation and water sorption are inherent physicochemical properties.[3] Psy and NaAlg are hydrophilic, biodegradable, biocompatible, and widely used materials in the pharmaceutical and food industries.[5] Problems of wear and tear on the composite microspheres (CMs) at high shear could be an issue for their mechanical stability.

The U.S. Department of Agriculture tried grafting an acrylonitrile polymer (resin) onto the backbone of starch molecules (starch grafting); this graft absorbed water more than 400 times its weight compared to pure starch, which was only able to retain water at 20 times its weight. Eventually, different vinyl monomers, such as acrylamide (AAm), *N-tert*-butyl acrylamide, methyl methacrylate, acrylonitrile, and methacrylamide, were chemically grafted on other natural polysaccharides to improve their sorption nature, stability, and physicochemical properties.[6,7] The grafting of polyacrylamide (PAM) onto polysaccharides was developed for its useful applications and is a subject of great interest.[8]

Crosslinked forms of PAM–polysaccharide have shown excellent resistance against degradation and have also been found to be stable. PAM is a well-known hydrophilic polymer; its high water retention and excellent swelling capability has gained considerable attention and wide use in materials for agricultural, sewage, and wastewater treatment; environmental friendly green technology; and biomedical and pharmaceutical applications.[6,7,9] PAM hydrogels are groups of three-dimensional (3D) interpenetrating networks made up of chemical interactions and crosslinkages of linear AAm monomer and are chemically known as poly(2-propenamide) or poly(1-carbamoylethylene). PAM mainly conjugates with its counterpart polymers via either

Table I. Composition of Different Batches for Fabrication of PAM-*g*-Psy–NaAlg CMs

Batch	NaAlg (mg)	Psy (mg)	AAm ($\times 10^{-1}$ mol/L)	MBA ($\times 10^{-3}$ mol/L)	APS ($\times 10^{-2}$ mol/L)	$NaHCO_3$ (mg)
PFT-1	300	50	2.89	9.72	1.09	100
PFT-2	300	100	2.89	9.72	1.09	100
PFT-3	300	150	2.89	9.72	1.09	100
PFT-4	300	150	1.45	19.45	1.09	100
PFT-5	300	150	2.89	19.45	1.09	100
PFT-6	300	150	4.35	19.45	1.09	100
PFT-7	300	150	2.89	29.18	1.09	100
PFT-8	300	150	2.89	19.45	0.547	100
PFT-9	300	150	2.89	19.45	2.18	100
PFT-10	300	150	2.89	19.45	1.09	50
PFT-11	300	150	2.89	19.45	1.09	150

hydrogen or covalent bonding; this results in the formation of an interpolymer complex.[10] Crosslinking between monomer units forms a unique 3D network (because of covalent bonding between monomers) that may give a strong mechanical strength.[11] Grafting is the most extensively studied and applied way to impose one's polymer chains onto another's backbone; it involves the growth of grafts directly onto the polysaccharide backbone.[4,12,13] The process involves free-radical polymerization; these free radicals can be conveniently created along the polysaccharide backbone in the presence of radical[14] or chemical initiators,[15] γ rays, UV radiation, electron beams,[16] and microwave irradiation.[4,7]

The squeezing capacity has been proposed to be an important parameter that can be used to understand the water squeezing ability of hydrogel networks under applied pressure. In this investigation, we grafted PAM onto polysaccharides to obtain CMs with improved mechanical strength. This study also dealt with the factors influencing the swelling, stability at high shear [Young's modulus (E)], and squeezing capacity of the prepared CMs.

EXPERIMENTAL

AAm was purchased from Merck Specialties Private, Ltd. (Mumbai India). *N,N*-methylene bisacrylamide (MBA) and ammonium persulfate (APS) were obtained from SISCO Research Laboratories Private, Ltd. (Mumbai, India). Psy and NaAlg were purchased from Indian Medicines Pharmaceutical Corp., Ltd., and Central Drug House (New Delhi, India), respectively. Sodium bicarbonate ($NaHCO_3$), anhydrous calcium chloride ($CaCl_2$), and hydrochloric acid (HCl) were procured from LOBA Chemie Pvt, Ltd. (Mumbai, India). All other chemicals were analytical grade and were used as obtained.

Scheme of Grafting

PAM gels were obtained by the crosslinking of the monomers (AAm) with a crosslinker (MBA) in a reaction preceded by initiators (APS). The properties of PAM strongly depend on the crosslinking of the monomers, crosslinkers, and initiators. The dilution of any one of them during the polymerization reaction affects the degree of grafting and the firmness of grafted network. Thus, the graft copolymers were synthesized through the grafting of PAM onto polysaccharides (NaAlg and Psy) by a free-radical polymerization method (Figure 1).[17] First, the aqueous solution of the monomer (AAm) was introduced into a polysaccharide mixture (2:1 NaAlg/Psy) in a beaker containing distilled water (10 mL) at a temperature of $30 \pm 2^{\circ}C$ under constant magnetic stirring (100 rpm) for 30 min (Table I).[18] Subsequently, the crosslinker (MBA), initiator (APS), and pore former ($NaHCO_3$)[19,20] were mixed at their respective molar concentrations for a reaction time of 4 h. Gelation and polymerization occurred after a prespecified time period and were followed by grafting.

Preparation of Composite Microspheres (CMs)

The polyacrylamide grafted psyllium-sodium alginate (PAM-*g*-Psy–NaAlg) polymeric mixture was homogenized and mixed thoroughly to obtain a very smooth, viscous, and pourable solution, which was transferred into a 19-G syringe. Under constant magnetic stirring, CMs were produced inside beakers, each of which contained gelation media. The gelation medium was prepared by the dissolution of $CaCl_2$ (4 g) into 100 mL of distilled water under constant magnetic stirring to obtain a transparent solution. Uniform, buoyant, porous, and spherical PAM-*g*-Psy–NaAlg CMs were instantly formed and were procured from acidified (with 1 mL of HCl added) gelation media (an inotropic gelation method).

Characterization

Fourier Transform Infrared (FTIR) Spectroscopy. Pellets of Psy, NaAlg, and PAM-*g*-Psy–NaAlg were prepared with potassium bromide (KBr) pellets containing 3% wt of materials. The FTIR spectra were recorded over the wave-number range 4000–500 cm^{-1} with a Shimadzu-8400S FTIR instrument (Japan).

Thermal Analysis. Thermal analysis measures both the heat flow and weight changes in a material as a function of the temperature or time under a controlled atmosphere. Differential scanning calorimetry (DSC) thermograms were recorded by the use of a DSC 2910-modulated DSC instrument (TA Instruments, New Castle, DE). DSC was calibrated with metallic indium (99.9% purity). The thermal analysis of Psy, NaAlg, and

Applied Polymer SCIENCE

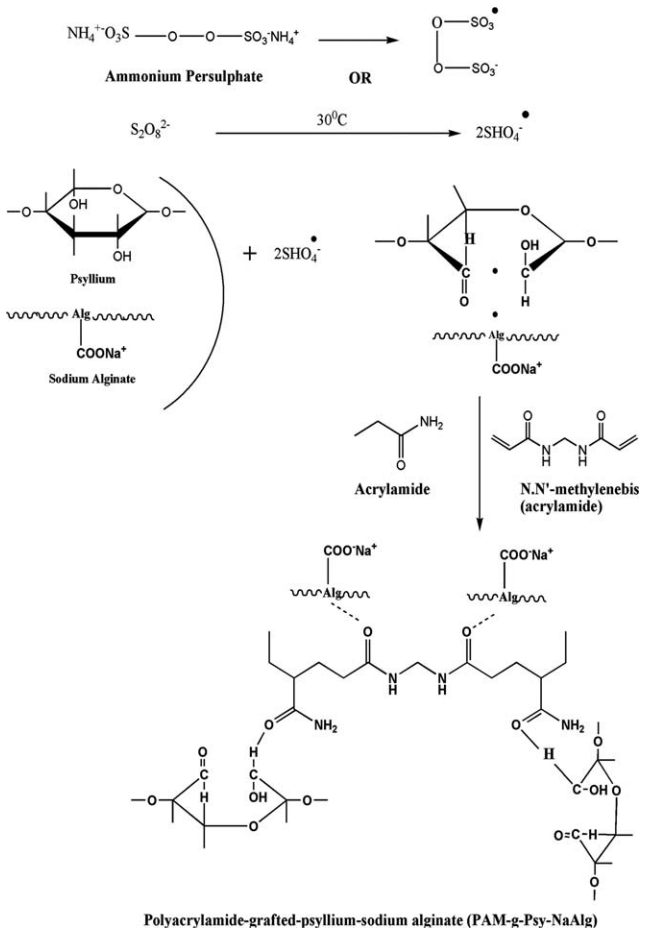

Figure 1. Scheme: Mechanism of graft co-polymerization reaction (drawn through *ChemDraw ultra 8.0* software)

PAM-*g*-Psy–NaAlg were tested in crimped aluminum pans at a heating rate of 20°C/min under dry N_2 gas (25 mL/min) over a temperature range from 30 to 450°C. The melting temperature was taken as the peak of the melting endotherm. The error in each measurement was estimated to be ±0.5°C in the examination of the thermal properties of the polymers.

Scanning Electron Microscopy (SEM). The morphological characteristics were observed with an environmental scanning electron microscope (Quanta 200). The PAM-*g*-Psy–NaAlg CMs were kept on a circular aluminum stub precoated with silver glue (to enhance the conductivity to electrons) and then observed under the scanning electron microscope at various magnifications, and micrographs were recorded. The samples were analyzed in SEM under high vacuum at 20 kV, and the detector used was a secondary electron detector.

Microsphere Diameter Measurement. The PAM-*g*-Psy–NaAlg CMs diameters were measured with digital vernier calipers (Absolute Digimatic, Mitutoyo Corp., Japan) with an accuracy of 0.001 mm. Individually, 20 CMs were subjected to diameter measurement, and an average was calculated.

Mechanical Strength. A new simple, in-house modified syringe method was developed in our laboratory, as shown in Figure 2, to measure the mechanical strengths of the PAM-*g*-Psy–NaAlg CMs. The device consisted of a 5-mL hypodermic Luer Mount borosilicate glass syringe (Perfektum, Hindustan Syringes Pvt, Ltd., Faridabad, India). From the delivery end, the needle hub was removed precisely from the main unit with glass cutter. The thumb rest was also opened from the upper end to make the plunger hollow and to pour mercury within it. Twenty wet CMs were placed under the syringe, and the syringe was placed vertically on a sieve (#40 mesh). The mercury was added dropwise within the hollow plunger. The weight of the mercury produced sufficient force for the movement of the plunger within the syringe, and the microspheres were pressed down. These PAM-*g*-Psy–NaAlg CMs were gradually compressed through predetermined compression loads of mercury (35, 60, 80, and 100 g) on the sieve. Prediametrical and postdiametrical changes of the microspheres were recorded with digital vernier calipers, and these values were used to calculate the mechanical strength.

Young's Modulus (E). E was used to measure the stiffness and observe behavior under pressure applied on the PAM-*g*-Psy–NaAlg CMs. In solid mechanics, the slope of the stress–strain curve at any point is called the *tangent modulus*. The tangent modulus of the initial or linear portion of a stress–strain curve is known as *Young's modulus*:

$$\sigma = \frac{F}{A}$$

$$\varepsilon = \frac{(d_w - d_c)}{d_w}$$

$$E = (F/A)/(\Delta d/d_w) = F d_w / A \Delta d$$

where σ is the tensile stress, F is the force, A is the area of the wet microsphere, ε is the tensile strain, d_w is the original diameter, d_c is the compressed diameter, and $\Delta d = (d_w - d_c)$ is the diametric difference of the PAM-*g*-Psy–NaAlg CMs.

Squeezing Capacity, Threshold Point, and Percentage Water Loss. A modified syringe method developed in-house was used to measure the squeezing capacity of the PAM-*g*-Psy–NaAlg CMs (Figure 2). An amount of 1 g of extemporaneous wet microspheres were placed under the syringe, which was placed vertically on a slab covered with tissue paper (which was used to wipe off excessive moisture). Mercury was added dropwise within the hollow plunger of the syringe (shown in Figure 2). The load of mercury was enough to produce sufficient force for the uniaxial movement of the plunger within the syringe. These CMs were gradually compressed by predetermined compression weight loads (35, 60, 80, and 100 g) of mercury on the slab. Excess water in the swollen PAM-*g*-Psy–NaAlg CMs was squeezed out under predetermined compression weight loads (water losses) and was readily absorbed by the tissue paper. The weight changes before and after treatment in the microspheres were recorded with a sensitive (least count ≤ 0.1 mg) electronic balance (Uni Bloc, Shimadzu Corp., Kyoto, Japan) used to calculate the squeezing capacity of the PAM-*g*-Psy–NaAlg CMs. The gradual loss of solvent from the microspheres under the application of a compression load reduced the microspheres' weight subsequently:

$$\text{Squeezing capacity} = (W_i - W_f) \times 100$$

$$Log\ S = Log\ \frac{W_i - W_f}{Wcl}$$

where W_i and W_f are the precompression and postcompression weights, respectively, of the PAM-*g*-Psy–NaAlg CMs, and W_{cl} is the applied compression weight load (weight of mercury; g).

RESULTS AND DISCUSSION

The grafting scheme demonstrated the reaction mechanism in which homolytic fission was involved in the dissociation of the initiator molecule (APS) and generated SO_4^- radicals as anions. Two SO_4^- anions were connected with the —O—O— bond (peroxide bond) and underwent breakdown under an aqueous environment to produce hydroxyl ions (Figure 1). We used these active SO_4^- anions further to initiate the polymerization process by pouring them into the beaker containing a viscous mucilaginous mixture of polysaccharide. The initiator (APS) generated free-radical sites on the polysaccharide (Psy and NaAlg) backbone and monomer; they were further crosslinked together in the presence of a multifunctional crosslinker (MBA). Thus, copolymerization followed by grafting of the PAM onto the polysaccharide produced a complex 3D network, which was termed the *PAM-grafted-Psy–NaAlg hydrogel network*.[17–20]

The alginates were easily converted into a gel in the presence of divalent (Ca^{++}) and trivalent cations (Al^{+++}). The chelation of the alginates and Psy through Ca^{++} ions gave a white color to the CMs.[21,22] Omidian et al.[21] explained that the formation of a lightly or tightly bound network occurred because of the exchange of the sodium ions of NaAlg with Ca^{++} ions and the consecutive stacking of guluronic groups in NaAlg. However, Guo et al.[22] reported that Ca^{++} ions significantly affect the gelling properties of Psy. They also claimed that changes in the elastic modulus of the gel were encountered with changes in the Ca^{++} ion concentration. The gel become more complex and dense with the addition of Ca^{++} ions, and thereafter, the fibrilous gel was converted into an aggregated gel. Thus, PAM-*g*-Psy–NaAlg grafted complex dimerized to form a gel network on the addition of Ca^{++} ions. Buoyancy was achieved because of the constant imbibition of HCl within the microspheres, which reacted with $NaHCO_3$ and liberated CO_2 gas. Furthermore, this CO_2 gas was easily entrapped within the complex network of microspheres and allowed the PAM-*g*-Psy–NaAlg CMs to float on the aqueous surface.[23]

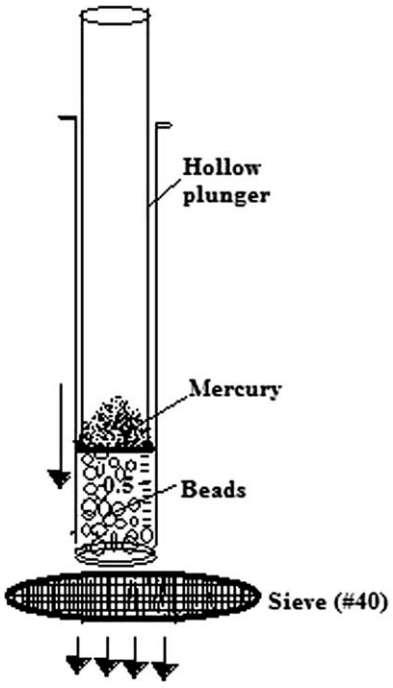

Figure 2. Schematic representation of *In-house developed modified syringe* method

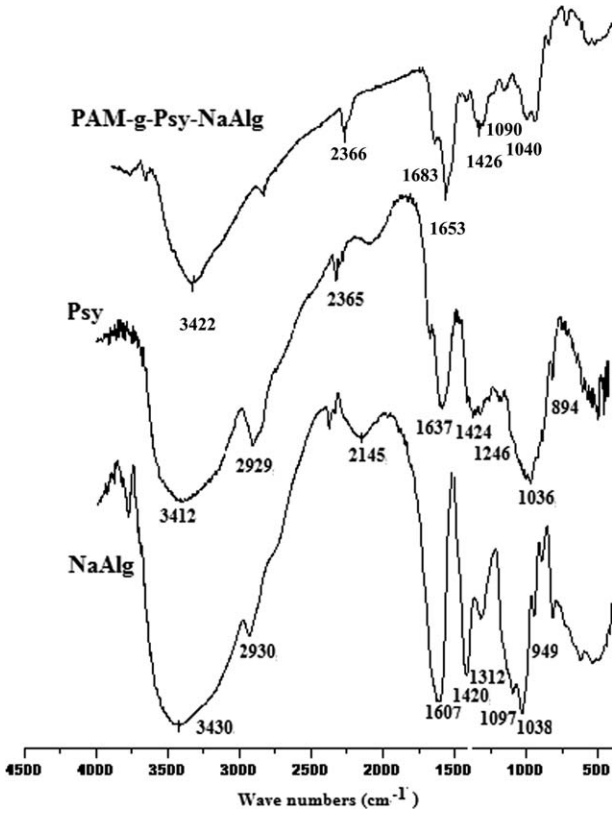

Figure 3. FTIR spectra of NaAlg, Psy, and PAM-*g*-Psy–NaAlg.

FTIR Studies

Figure 3 shows the FTIR spectra of NaAlg, Psy, and PAM-*g*-Psy–NaAlg. A broad stretching band at 3430 cm^{-1} appeared because of the —OH groups of NaAlg. The absorption band present at 2929 cm^{-1} was due to —CH vibrations in NaAlg and Psy.[24,25] Further, in the NaAlg spectra, the appearance of absorption bands at 1607 and 1420 cm^{-1} were due to —COO groups.[24] The stretching bands present at 1097 and 1038 cm^{-1} confirmed the presence of —C—O groups in NaAlg.

In the FTIR spectra of Psy, the respective broad bands at 3412 and 2930 cm^{-1} were due to —OH stretching and —CH vibrations, respectively, for arabinose, xylose, and traces of other sugars present in Psy. The stretching band appearing at 894 cm^{-1} was due to the vibration of the pyranose ring, whereas the characteristic bands between 1246 and 1036 cm^{-1} were due to

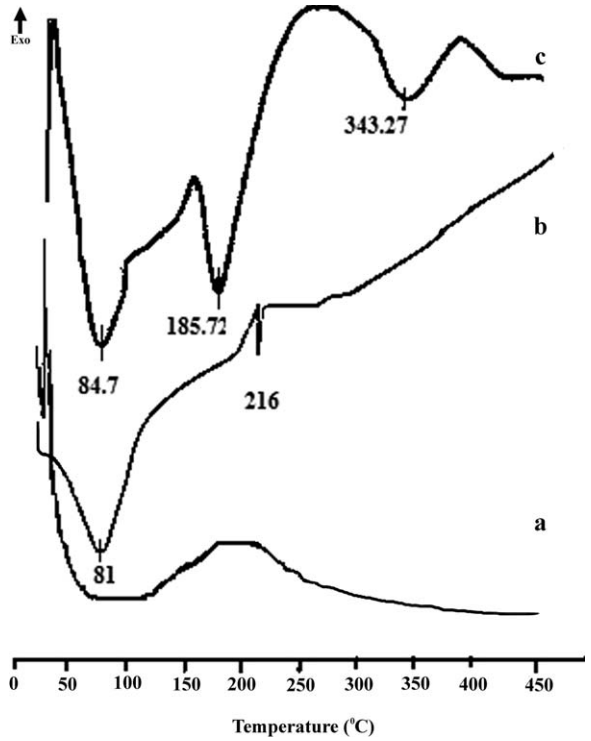

Figure 4. Thermal analyses: (a) Psy, (b) NaAlg, and (c) PAM-*g*-Psy–NaAlg.

—C—O and —C—O—C vibrations of the Psy's polysaccharide.[21,26]

In the FTIR spectra of PAM-*g*-Psy–NaAlg, the absorption band appearing at 3422 cm^{-1} revealed the overlap of the —NH stretching band of amide groups along with the —OH groups of the polysaccharide due to grafting. The absorption band at 2366 cm^{-1} confirmed the presence of Psy in PAM-*g*-Psy–NaAlg. Furthermore, appearance of bands at 1683 and 1426 cm^{-1} were due to the —CO and —NH stretching of amide I and amide II, respectively.[25,27] The absorption peaks appearing between 1000 and 1100 cm^{-1} confirmed the ether (C—O—C) linkages present in the polysaccharides (NaAlg, Psy, and PAM-*g*-Psy–NaAlg) and were least interfering. The band at 941–820 cm^{-1} again showed the vibration of the pyranose ring of polysaccharide present in PAM-*g*-Psy–NaAlg.[26] Thus, the FTIR results revealed the successful grafting of PAM onto Psy and NaAlg to form the PAM-*g*-Psy–NaAlg composites.

Thermal Analysis

The glass-transition temperatures (T_g) were used to describe chain segmental motion. The thermal analysis graph (Figure 4) revealed that the initial T_g of NaAlg was found to be 81°C, whereas in PAM-*g*-Psy–NaAlg CMs, T_g was 84.72°C.[2,28]

This slight shift in T_g toward the upper temperature range explained the restricted segmental mobility of NaAlg within PAM-*g*-Psy–NaAlg. NaAlg is a polysaccharide that consists of two hydroxyls and one carboxylate segment at every repeating unit and has α and β configurations. During grafting, chain entanglement would occur between the hydroxyl groups of NaAlg and the carboxyl groups of PAM.[4]

Furthermore, the PAM-*g*-Psy–NaAlg CMs showed three different characteristic endothermic peaks at 84.72, 185.72, and 343.27°C, respectively. The melting of NaAlg at 216°C might have converted these into two melting endotherms at 185.72°C (early) and 343.27°C (late). This shift in the melting endotherm of NaAlg in the PAM-*g*-Psy–NaAlg CMs was the result of interactions between the carboxyl groups of NaAlg and the ethereal oxygen of PAM and was also due to the chain entanglement of Psy with NaAlg. This amplification in T_g indicated the restricted segmental mobility of Psy with NaAlg in the grafted PAM-*g*-Psy–NaAlg CMs.[28]

Effect of the Variables on the Diameter and Swelling

The microsphere diameter was used as a function to measure the swelling. Through our preliminary investigation, we observed that varying the concentrations of the monomer, initiator, and crosslinker and other environmental factors (pH, temperature, and ionic strength) severely affected the diameter and swelling. The graft copolymerization induced polymer chains of different characteristics, depending on the concentration of reactants were added. The degree of polymerization and grafting directly affected the chain length, thickness, rigidity, and overall diameter of the CMs. Thus, in this article, we briefly describe the comparative concentration-dependent effect of the monomer, crosslinker, initiator, and pore former (with a constant polysaccharide amount) on the swelling, *E*, mechanical strength, and squeezing capacity of the grafted microspheres.

Monomer. A sequential decrement in the microsphere's diameters were observed among the batches (PFT-4 > PFT-5 > PFT-6: 4.17 > 3.76 > 3.37 mm) with the gradual increase in monomer (AAm) concentration. As the monomer concentration was increased, the production of new polymeric chains and their elongation were helped, but the swelling of the CMs deteriorated (Figure 5).[29,30] At a low concentration of monomer (PFT = 1.45 × 10^{-1} mol/L), the free available space between the chains was expected to be quite large; thus, it produced bigger microspheres. However, a gradual increase in the monomers (the concentrations of PFT-5 and PFT-6 were

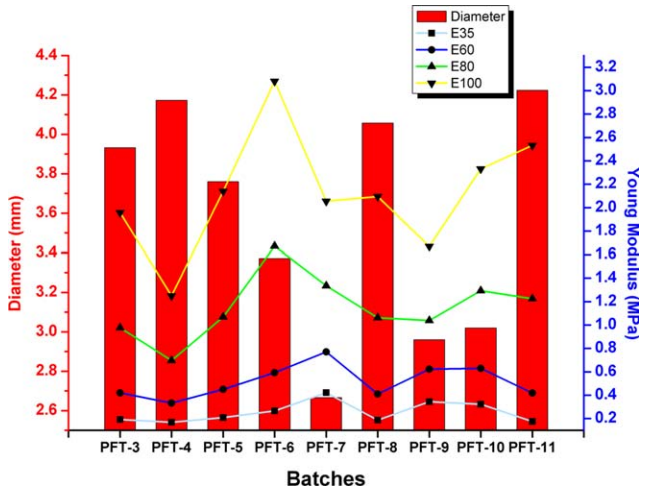

Figure 5. Diameter (swollen state) and *E* values of different batches of PAM-*g*-Psy–NaAlg CMs. [Color figure can be viewed in the online issue, which is available at www.interscience.wiley.com.]

4.35 and 2.89 $\times$ 10^{-1} mol/L, respectively) led to the propagation of the chain length and self-crosslinking; hence, this reduced the available free space between the two chains and produced small microspheres (the diameters of PFT-5 and PFT-6 were 3.961 and 3.334 mm, respectively; Figure 5).[26,31,32]

Crosslinker. Increases in the crosslinker concentration (PFT-3 < PFT-5 < PFT-7: 9.72 < 19.45 < 29.18 $\times$ 10^{-3} mol/L) were attributed to decreases in the microsphere diameter (3.93 > 3.76 > 2.66 mm) due to complex network formation (Figure 5). The crosslinker (MBA) played a crucial role in the polymerization, and a small amount of crosslinker was sufficient for the transition of the liquid to a gel state during the synthesis of the PAM-*g*-Psy–NaAlg CMs.[32] Crosslinkers have the unique ability to interlock two or more monomer units together and sometimes multiple interlocking at specific positions to form an intertwined structure. PFT-7 showed the least diameter (2.66 mm) among all of the CM batches. An increase in the crosslinker concentration enhanced the crosslinked density, but consequently, the pore sizes of the network decreased; this did not support the entrapment of more water inside the network (reduced swelling; Figure 5).

Initiator. Figure 5 shows that the microsphere diameter decreased rapidly (4.05 > 3.76 > 2.96 mm) with increasing initiator (APS) concentration (PFT-8 > PFT-5 > PFT-9: 0.547 > 1.09 > 2.18 $\times$ 10^{-2} mol/L). The initiator acted as a catalyst and initiated the graft copolymerization reaction. The initiator decomposed itself into free radicals in the presence of monomers and favored the chemical process (polymerization or crosslinking) by providing the reaction site. Its decomposition was a rate-determining step of the polymerization process. As the polymerization reaction proceeded, it again favored the crosslinking and grafting processes (Figure 1). A low concentration of the initiator (APS) left abundant monomers (AAm) and crosslinkers (MBA) in the unpolymerized state and thereby produced a less intertwined network. However, their large concentration had a negative impact on the polymer performance (mechanical strength and swelling capacity) because of the high rigidity of the grafted network.[33] It is important to note that the synthesis of the PAM-*g*-Psy–NaAlg hydrogel progressed because of the chemical and physical crosslinking of the linear polymer chains of PAM with the polysaccharide's chains and their reintertwinement together. Long polymer chains of PAM entwined better to form a complex hydrogel network compared to the short chains of the polysaccharides. Thus, linear or branched polymer chains moved inside the grafted network, performing wormlike motions called *reptation* and restricted the free molecular motion of other chains.[34]

Pore Former. We observed that as the concentration of the pore former ($NaHCO_3$) was increased (PFT-10 < PFT-5 < PFT-11), the diameter (3.01 < 3.76 < 4.22 mm; Figure 5) of the CMs increased. The pore former expanded these microspheres internally because of CO_2 gas, and the microsphere became bigger in size. The PFT-11 microspheres were the biggest in size (4.22 mm). The porosity and buoyancy could be achieved because of the continuous imbibitions of HCl in the $NaHCO_3$ (pore former) loaded microspheres. The reaction liberated CO_2 as a byproduct. Furthermore, this CO_2 gas get entrapped within the complex grafted network and allowed the PAM-*g*-Psy–NaAlg CMs to remain afloat at the top of the aqueous surface.[23] The buoyancy was added as an advantageous feature for easy evacuation or wipeout of these microspheres from any aqueous surface versus that of sunken microspheres.

To verify the sequences of pore formation inside the PAM-*g*-Psy–NaAlg CMs, the cross section of different batches, PFT-10, PFT-5, and PFT-11, of microspheres with a gradual increase in their pore-former concentration were briefly evaluated through SEM analysis (Figure 6). Bulges, fractures, and fewer pores were observed in the cross section of PFT-10 compared with those of PFT-5 (which seemed to be more porous) and PFT-11 (abrupt macrosized pores). Macrosized pores revealed that more CO_2 were produced in the PFT-11 CMs (which had the highest concentration of pore former). The macrosized pores of PFT-11 allowed greater water accumulation inside CMs, but their mechanical strength suffered severely compared to PFT-5 and PFT-10. A greater amount of $NaHCO_3$ in the mixture produced more CO_2, which turned into multiple perforations within the PAM-*g*-Psy–NaAlg CMs network.

More CO_2 gas was the reason behind increases in the microsphere diameter because it built a constant internal pressure for their expansion. However, pressure escaped readily through the tiny pores of the grafted network and left the microspheres deflated after a brief size expansion (Figure 6). The internal pressure in the microsphere was attributed the multidimensional breakage of the hydrogel network (CO_2 gas escaped through ruptures in the grafted network and the breaking of their chains). Thus, the microspheres of batch PFT-11 had the biggest diameter among all of the microsphere batches (Figure 5).[19]

Mechanical Strength and *E*

The mechanical properties and deformation rate are interdependent features. The PAM-*g*-Psy–NaAlg CMs exhibited elastomeric–mechanical properties because of their hydrogel nature, and these could be determined by various methods. *E* is one useful parameter for measuring the mechanical strength and rigidity (stiffness) of such hydrogels. It has been reported that more would be E, greater be its mechanical strength.[9]

At 35 and 60 g of compression weight load, the microspheres of the PFT-7 batch showed the highest *E* ($E_{35} = 0.422$ and $E_{60} = 0.77$ MPa) among all of microspheres (Figure 5). Surprisingly, with gradual increases in the compression weights to 80 and 100 g, the highest *E* value shifted toward the PFT-6 ($E_{80} = 1.67$ and $E_{100} = 3.08$) batch from PFT-7 ($E_{80} = 1.33$ and $E_{100} = 2.05$). This observation give a clear indication that the mechanical strength, stiffness, and rigidity of the network were affected either by the monomer (PFT-6) or crosslinker (PFT-7). Our findings were similar to those of Martínez-Ruvalcaba et al.,[9] in which an increase in the crosslinking density resulted in a reduction in the swelling capacity and an increment in *E* (PFT-6 and PFT-7). As the concentration of the monomers (PFT-4 < PFT-5 < PFT-6), crosslinkers (PFT-3 < PFT-5 < PFT-7), and initiators (PFT-8 < PFT-5 < PFT-7) gradually increased

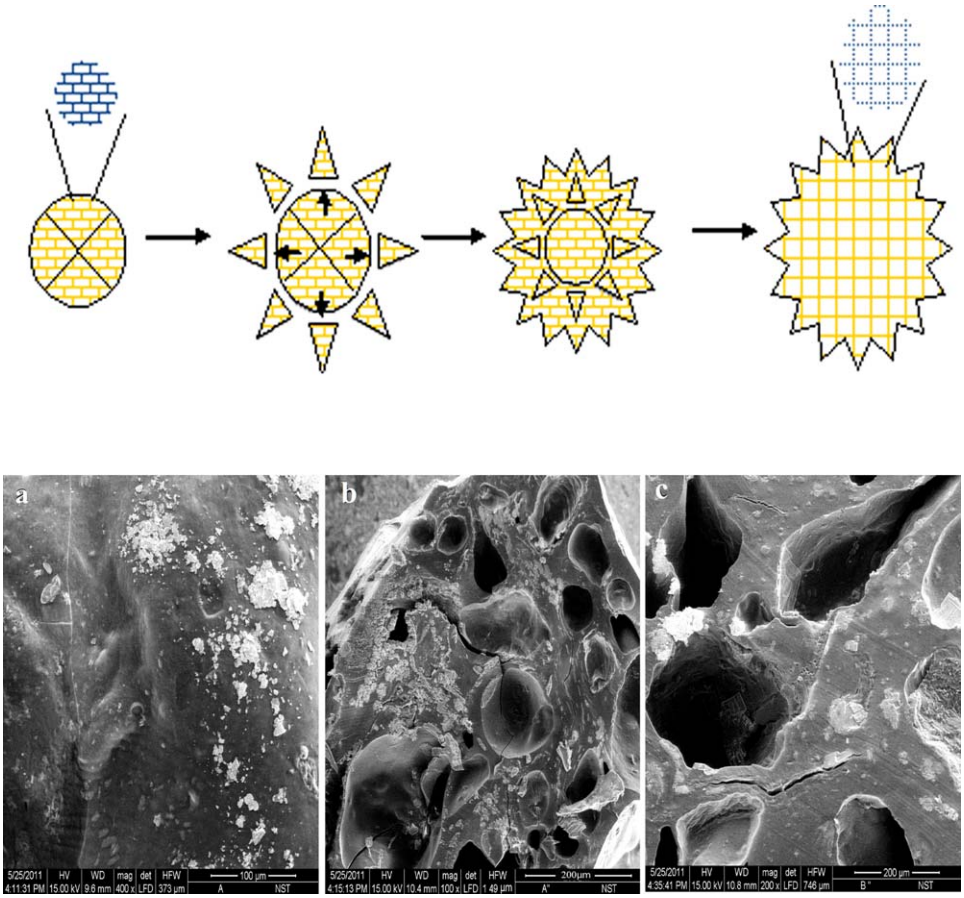

Figure 6. Schematic representation of the unfastening of the CM network due to the formation of CO_2 gas and SEM photographs of a cross section of the PAM-*g*-Psy–NaAlg CMs: (a) PFT-10, (b) PFT-5, and (c) PFT-11. [Color figure can be viewed in the online issue, which is available at www.interscience.wiley.com.]

and the other factors were kept to a constant amount; an exponential increase in *E* was observed at each compression weight load (35, 60, 80, and 100 g; Figure 5). High grafting and crosslinking led to greater mechanical strength; thus, PAM imparted strong elastomeric properties to the polysaccharide backbone. The mechanical strength of the microspheres was variable and dependent on various other factors. The coil-like pattern of PAM represents the hydrophobic part of the PAM-*g*-Psy–NaAlg hydrogel, whereas the chainlike conformations in the grafted hydrogels were due to the hydrophilic portions of Psy and NaAlg.[34] The coil-like hydrophobic conformations of the PAM-*g*-Psy–NaAlg hydrogel due to the presence of PAM endowed essential elastomeric and mechanical properties to the grafted network under stress conditions.

The overall decrease in the microsphere's diameter strengthened the mechanical strength of the CMs. The strong and stiff PAM-*g*-Psy–NaAlg hydrogel repelled the applied load more promisingly than the loosely bonded network. A highly crosslinked network would resist structural deformation so the elastic nature of the grafted hydrogel gave additional strength to the PAM-*g*-Psy–NaAlg networks. PFT-7 showed the smallest microspheres, in which the concentration of the crosslinker was highest; thus, the crosslinker strengthened the networks through more bonding or interlocking between the monomers, polysaccharide, and PAM. The crosslinker interfered with the mobility of the polymer chain,[35] and the initiator sped up the grafting and polymerization reaction.

Squeezing Capacity and Percent Water Loss

The squeezing capacity test was carried out by the exertion of compressive load on the microspheres, and this expelled water. The maximum point at which these CMs resisted the load applied against their diametrical change was known as the *threshold point*. The threshold point is the function of Log *S* versus the compression load plot. The logarithm of squeezing versus the compression load and percentage water loss versus the compression load are plotted in Figure 7(a–d). However, *squeezing before collapse* was the point at which the structural deformation of microspheres took place after the complete removal of water through it. Squeezing before collapse was a function of the amount of water lost, was complementary to the threshold point, and appeared at similar compression weight loads for each batch. The squeezing capacity of the microspheres was inversely related to the mechanical strength.

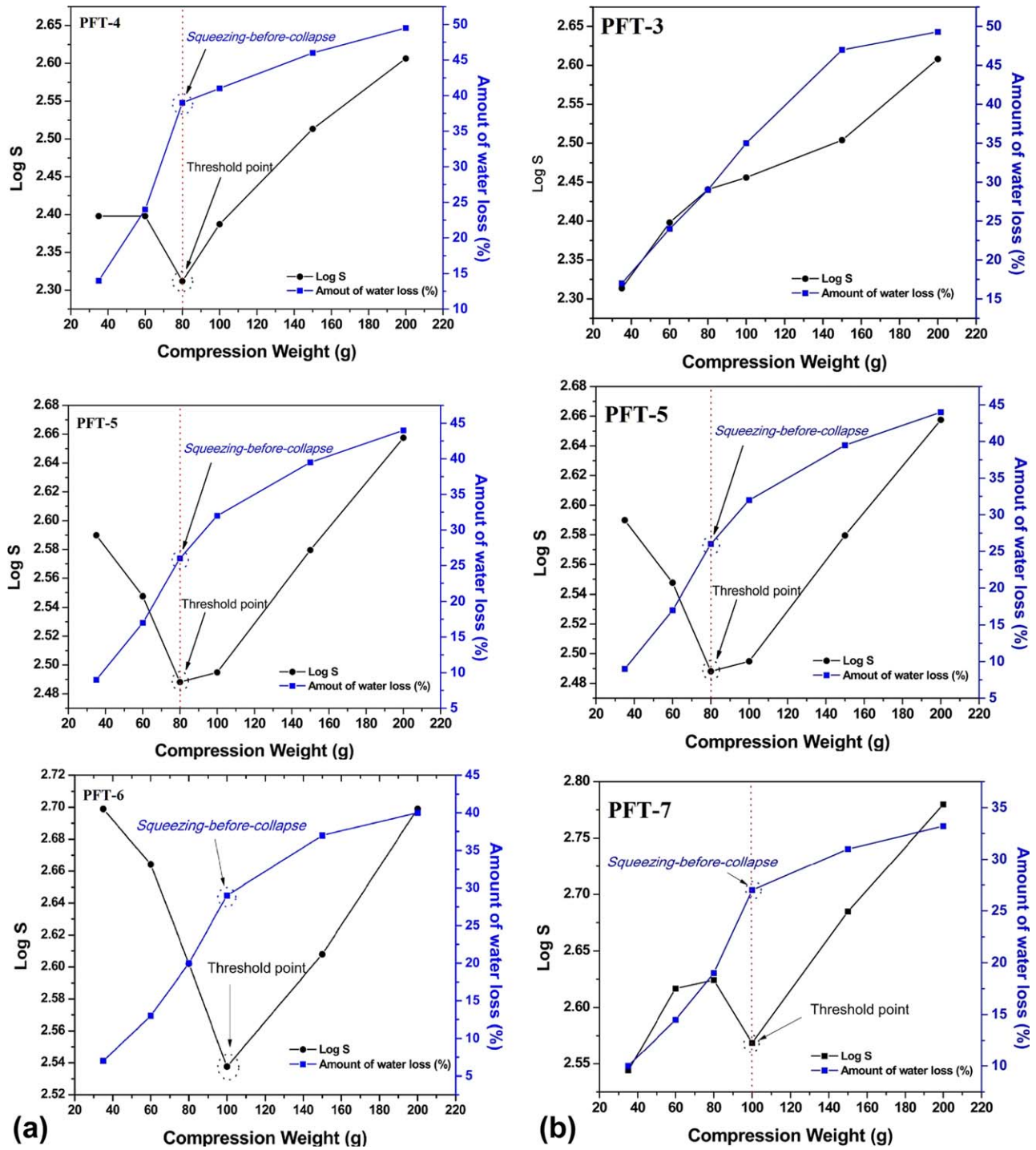

Figure 7. Squeezing capacity and percentage water squeezed out from different batches of PAM-*g*-Psy–NaAlg CMs with the enhancement of the (a) monomer (AAm) concentration, (b) crosslinker (MBA) concentration, (c) initiator (APS) concentration, and (d) pore former ($NaHCO_3$) concentration. [Color figure can be viewed in the online issue, which is available at www.interscience.wiley.com.]

The threshold points (Log *S* values) of the PFT-4, PFT-5, and PFT-6 CMs were found to be 2.31, 2.48, and 2.53 at 80, 80, and 100 g, respectively, of compression weight [Figure 7(a)]. Swelling was highest for the microspheres (PFT-4) prepared with the lowest monomer (AAm) concentration (Figure 5). The shifting of the highest threshold point toward a high compression load with gradual increases in monomer (AAm) concentration explained the improvement in the network mechanical strength (Table I). At the threshold point, all of the PAM-*g*-Psy–NaAlg CMs resisted further increases in the operational load; thus, the rate of solvent ejection became low thereafter.[29,36,37] As shown in Figure 7(a), with increases in the gradual compression weight load (35, 60,

Applied Polymer SCIENCE

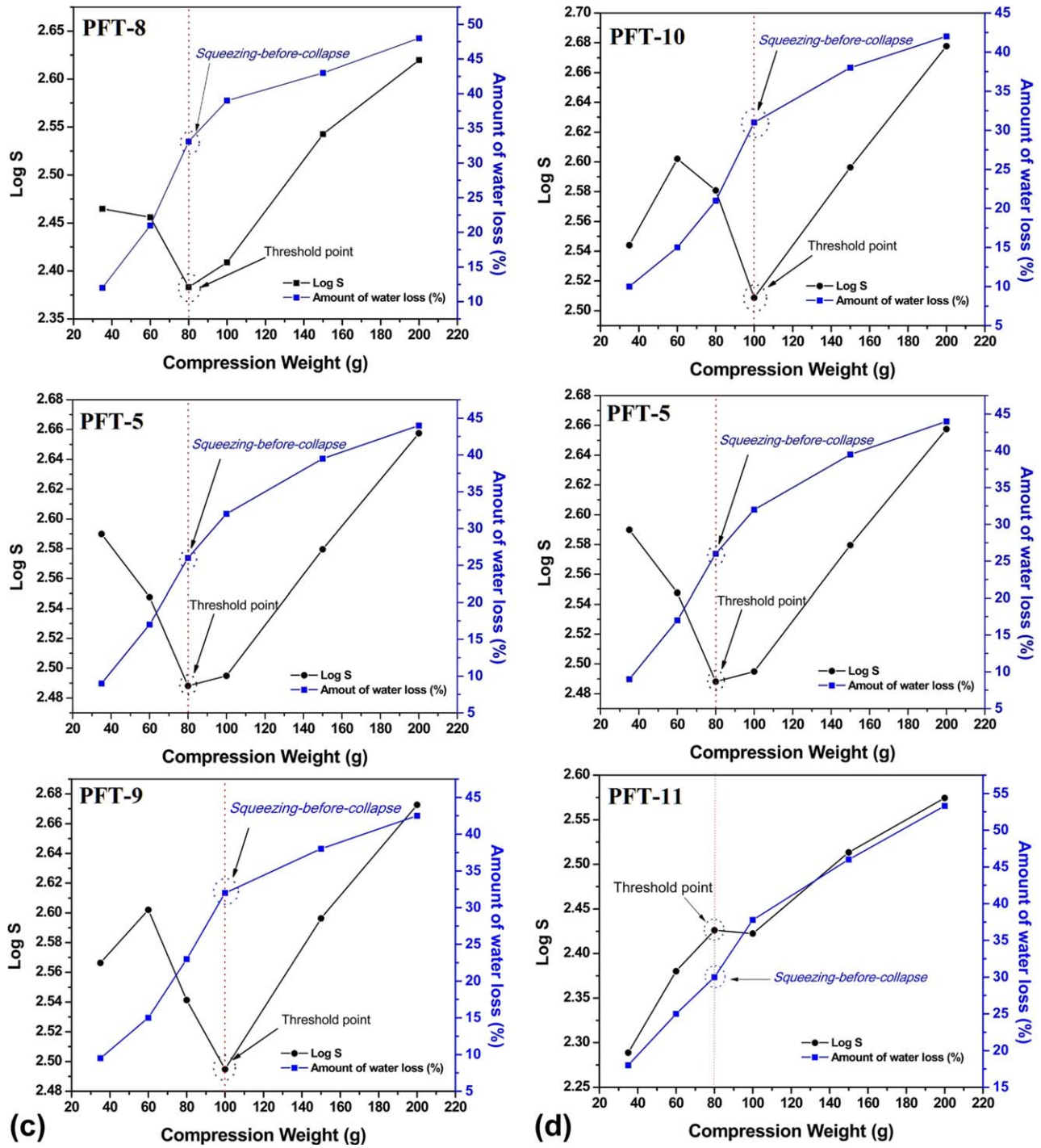

Figure 7. (Continued).

and 80 g), the PFT-4 batch was able to easily squeeze water out from its less complex CM network compared to the more complex and interwoven networks (PFT-5 and PFT-6). The amounts of water squeezed out at the squeezing-before-collapse point for PFT-4, PFT-5, and PFT-6 were 39, 26, and 29%, respectively, whereas at 200 g (the highest compression load), the total water squeezed from the microspheres was found to gradually lessen (PFT-4 < PFT-5 < PFT-6: 49.5 > 44 > 40%) with increasing monomer concentration. A substantial improvement in the mechanical strength of the grafted network was achieved, which reduced its squeezing capacity.

The threshold points (Log *S* values) of PFT-3, PFT-5, and PFT-7 were found to be no threshold, 2.48, and 2.56 at 0, 80, and 100 g, respectively, of compression weight [Figure 7(b)].[15] A shift in the threshold point toward a higher weight load from 0 to100 g was observed with the gradual increase in the crosslinker (MBA) concentration (Table I). As the concentration of crosslinker was increased (PFT-3 < PFT-5 < PFT-7), the water

squeezed at 200 g (highest weight load) was found to decrease [49.3 > 44 > 33.2%; Figure 7(b)]. This revealed that the soft or thin swollen polymeric CMs of PFT-3 could eject more solvent and collapsed easily under a lesser weight load compared to the inflexible and complex microspheres (PFT-5 and PFT-7). The amounts of water squeezed out at the squeezing-before-collapse point for PFT-3, PFT-5, and PFT-7 were found to be 0, 26, and 27%, respectively. Grafting and crosslinking abridged the space available to hold water; thus, the overall swelling subsided and was followed by an improvement in the mechanical strength. An increase in the crosslinker concentration enhanced the grafting and crosslinking greatly and thereby allowed less water to be squeezed out in inflexible and complex networks of the PAM-*g*-Psy–NaAlg CMs.[31,38]

The threshold points (Log *S* values) of the PFT-8, PFT-5 and PFT-9 CMs were found to be 2.38, 2.48, and 2.49 at 80, 80, and 100 g, respectively, of compression weight load [Figure 7(c)]. Again, a shift in the highest threshold point toward a higher compression load with a gradual increase in the initiator (APS) concentration was observed (Table I). The amounts of water squeezed out at the squeezing-before-collapse point for PFT-8, PFT-5, and PFT-9 were 33.1, 26, and 32%, respectively. Subsequently, a gradual decrease in the total water squeezed from the microspheres was also observed (48 > 44 > 42.5%) at 200 g (the highest compression load). Increments in the initiator concentration led to the formation of more macromolecular chains and, therefore, a reduction in the free volume of the network.[31] Further, the microspheres of the weakly crosslinked network (PFT-8) had better squeezing rates because more water was expelled at lower compression loads compared to that in the more densely formed microspheres of PFT-9 (with better mechanical strength), which squeezed at a higher compression load.

The highest threshold points for PFT-10, PFT-5, and PFT-11 were found to be 2.5, 2.48, and 2.42 at 100, 80, and 80 g of weight, respectively. A decrease in the highest threshold point toward a lesser compression weight load with the gradual increase in pore former ($NaHCO_3$) concentration (Table I) was observed [Figure 7(d)]. In contrast to the monomer, crosslinker, and initiator effect, as the concentration of pore former was increased (PFT-10 < PFT-5 < PFT-11), this resulted in an improvement in the maximum amount of water squeezed from the microspheres (42 < 44 < 53.3%) at 200 g [the highest compression load; Figure 7(d)], whereas the amounts of water squeezed out at the squeezing-before-collapse point for PFT-10, PFT-5, and PFT-11 were 31, 26, and 30%, respectively. The reason behind this observation was that more CO_2 gas was formed as the concentration of $NaHCO_3$ was increased. The escape of CO_2 gas was due to the porous network; thus, the microspheres were flexible enough to squeeze out more water (Figure 6). Broken polymeric chains and a disintegrated network rendered poor mechanical strength to the deflated PFT-11 microspheres. Thus, the microspheres of PFT-11 held a diminished mechanical strength and a fairly high squeezing capacity among all of the grafted CMs.

Swelling is a specific feature that can be extensively used to characterize the strength of polymer networks. The high water uptake at a low degree of crosslinking for semi-interpenetrating polymer network microspheres of AAm grafted onto dextran and chitosan prepared by emulsion–crosslinking was already reported.[39] The threshold point revealed that a water squeezing rate greater with respect to the load applied until the collapse of the microspheres (squeezing before collapse) was not observed. The threshold point and squeezing before collapse was the resistance mark at which polymeric network was able to repel (aversion) the weight load applied on it and was able to squeeze out the maximum amount of water. At zero threshold, the grafted networks were not able to show elastomeric behavior and squelched promptly upon compression load without resisting it. Initially, the swollen grafted networks behaved like soft porous sponges, and subsequently, they squeezed water out as the compression weight load was increased (the swollen chains of the network came close to each other and thereby squeezed water out that was present between the chains).

CONCLUSIONS

The previous discussion suggests the successful grafting of PAM onto polysaccharides. Loosely crosslinked CMs (PFT-3 and PFT-11) collapsed more easily than complex and strongly bonded crosslinked CMs. More interwoven crosslinked networks of the PAM-*g*-Psy–NaAlg CMs (PFT- 4, PFT-5, PFT-6, PFT-7, PFT-8, and PFT-9) held some elastomeric properties to restore the networks easily at their threshold point, after which their diametrical collapse became irreversible and their microspheres were squashed.

The aggregations of grafted chains prevented complex network formation and also crosslinking within the CMs. When the concentrations of monomer, crosslinker, and initiator were low, these grafted chains were flexible enough to accommodate large amounts of water within, and thus, they could squeeze more water out. However, the complex interlocking of chains at higher concentrations resulted in a decrease in the overall network space, and they squeezed less water out because of to low hydration. Furthermore, graft copolymerization improved the mechanical strength of the PAM–polysaccharide network, and the complex interwoven network resisted more against the applied weight load and failed to squeeze more (a low squeezing capacity). The flexibility of the network played a critical role in the squeezing. In general, this phenomenon is just like the squeezing of a soft sponge compared to that of a harder one. *E* of crosslinked PAM-*g*-Psy–NaAlg CMs were enhanced with the progress of graft copolymerization.

The grafting of PAM onto polysaccharides is a new avenue to explore for grafting technology to improve and impose a variety of useful properties onto other polymers. Such grafted PAM-*g*-Psy–NaAlg microsphere carriers possess excellent mechanical strength and resistance under high shear, which would certainly be beneficial to their application in different fields, including ecofriendly environmental municipal remediation, agriculture, polymer science, petroleum industry, smart drug delivery, and wastewater management.

ACKNOWLEDGMENTS

One of the authors (R.T.) is thankful to Indian Council of Medical Research (ICMR), New Delhi, India, for the Senior Research Fellowship (SRF) award. The authors are thankful to O. N. Srivastava,

Department of Physics, Banaras Hindu University (BHU), for SEM analysis; the University Grant Commission-Department of Atomic Energy (UGC-DAE) Consortium for Scientific Research, Indore; and the Department of Ceramic Engineering, Indian Institute of Technology (IIT)–BHU, for thermal analysis. The authors wish to thanks to Mrs. Shraddha Singh, Research Scholar, School of Material Science and Technology, IIT–BHU, for useful suggestions in the development of the modified syringe device.

REFERENCES

1. Craeyveld, V. V.; Delcour, J. A.; Courtin, C. M. *Food Chem.* **2009**, *11*, 812.
2. Edwards, S.; Chaplin, M. F.; Blackwood, A. D.; Dettmar, P. W. P. *Nutr. Soc.* **2003**, *62*, 217.
3. Fischer, M. H.; Yu, N. X.; Gray, G. R.; Ralph, J.; Anderson, L.; Marlett, J. A. *Carbohydr. Res.* **2004**, *339*, 2009.
4. Mruthyunjayaswamy, T. M.; Ramaraj, B.; Siddaramaiah. J. *Macromol. Sci. A* **2010**, *47*, 877.
5. Singh, V.; Kumar, P.; Sanghi, R. *Prog. Polym. Sci.* **2012**, *37*, 340.
6. Kasgöz, H.; Durmus, A. *Polym. Adv. Technol.* **2008**, *19*, 838.
7. History of Super Absorbent Polymer Chemistry. http://www.m2polymer.com/html/history_of_superabsorbents.html. (accessed June 1, **2012**).
8. Athawale, V. D.; Rathi, S. C. *J. Macromol. Sci. Polym. Rev.* **1999**, *39*, 445.
9. Martínez-Ruvalcaba, A.; Sánchez-Díaz, J. C.; Becerra, F.; Cruz-Barba, L. E.; González-Álvarez, A. *eXPRESS Polym. Lett.* **2009**, *3*, 25.
10. Krusicel, K. M.; Dzunuzovic, E.; Trifunovic, S.; Filipovi, J. *Polym. Bull.* **2003**, *51*, 159.
11. Joshy, M. I. A.; Elayaraja, K.; Suganthi, R. V.; Kalkura, N. *Cryst. Res. Technol.* **2010**, *45*, 551.
12. Butler, C. E.; Millington, C. A.; Clements, D. W. G. In Historic Textile and Paper Materials II; Hansen, E. F., Ginell, W. S., Zeronian, S. H., Eds.; Oxford University Press: Oxford, United Kingdom, **1989**.
13. Princi, E.; Vicini, S.; Pedemonte, E.; Arrighi, V.; McEwen, I. J. *J. Appl. Polym. Sci.* **2007**, *103*, 90.
14. Code, K. R. U.S. Pat. 0,296,883A1 (**2011**).
15. Xu, F. J.; Kang, E. T.; Neoh, K. G. *Biomaterials* **2006**, *27*, 2787.
16. Robinette, E. J.; Palmese, G. R. *Nucl. Instrum. Methods B* **2005**, *236*, 216.
17. Mishra, A.; Rajani, S.; Agarwal, M.; Dubey, R. P. *Polym. Bull.* **2002**, *48*, 439.
18. Gelfi, C.; Righetti, P. G. *Electrophoresis* **1981**, *2*, 220.
19. Park, K.; Chen, J.; Park, H. U.S. Pat. 6,271,278 (**2001**).
20. Singh, B.; Chauhan, N. *Food Hydrocolloid* **2009**, *23*, 928.
21. Omidian, H.; Rocca, J. G.; Park, K. *Macromol. Biosci.* **2006**, *6*, 703.
22. Guo, Q.; Cui, S. W.; Wang, Q.; Goff, H. D.; Smith, A. *Food Hydrocolloid* **2009**, *23*, 1542.
23. Khan, Z. A.; Tripathi, R.; Mishra, B. *AAPS PharmSci.* **2011**, *12*, 1312.
24. Tripathy, T.; Pandey, S. R.; Karmakar, N. C.; Bhagat, R. P.; Singh, R. P. *Eur. Polym. J.* **1999**, *35*, 2057.
25. Sen, G.; Pal, S. *Int. J. Biol. Macromol.* **2009**, *45*, 48.
26. Singh, B.; Sharma, V. *Int. J. Pharm.* **2010**, *389*, 94.
27. Kulkarni, R. V.; Sa, B. *Drug Dev. Ind. Pharm.* **2008**, *34*, 1406.
28. Soares, J. P.; Santos, J. E.; Chierice, G. O. E.; Cavalheiro, T. G. *Ecl. Quím. São Paulo* **2004**, *29*, 53.
29. Kumar, K.; Kaith, B. S.; Jindal, R.; Mittal, H. *Appl. Polym. Sci.* **2012**, *124*, 4969.
30. Escobar, J. L.; Aguero, L.; Zaldivar, D.; Katime, I.; Rodriguez, R. E. *Rev. Iberoam. Polim.* **2001**, *2*, 40.
31. Bajpai, A. K.; Giri, A. *Carbohydr. Polym.* **2003**, *53*, 271.
32. Singh, B.; Chauhan, G. S.; Bhatt, S. S.; Kumar, K. *Carbohydr. Polym.* **2006**, *64*, 50.
33. Mijangos, I.; Navarro-Villoslada, F.; Guerreiro, A.; Piletska, E.; Chianella, I.; Karim, K.; Turner, A.; Piletsky, S. *Biosens. Bioelectron.* **2006**, *22*, 381.
34. Kozhunova, E. Y.; Makhaeva, E. E.; Khokhlov, A. R. *Polymer* **2012**, *53*, 2379.
35. Singh, B.; Chauhan, G. S.; Kumar, S.; Chauhan, N. *Carbohydr. Polym.* **2007**, *67*, 190.
36. Pourjavadi, A.; Mahdavinia, G. R. *Turk. J. Chem.* **2006**, *30*, 595.
37. Mina, A. F.; Alam, M. A. *Chin. J. Polym. Sci.* **2005**, *23*, 269.
38. Bajpai, A. K.; Bajpai, J.; Shukla, S. *React. Funct. Polym.* **2001**, *50*, 9.
39. Rokhade, A. P.; Patil. S. A.; Aminabhavi, T. M. *Carbohydr. Polym.* **2007**, *67*, 605.